Unexpected changes in community size structure in a natural warming experiment

Eoin J. O'Gorman[1,*,†], Lei Zhao[2,1,†], Doris E. Pichler[3], Georgina Adams[1], Nikolai Friberg[4], Björn C. Rall[5,6], Alex Seeney[3], Huayong Zhang[2], Daniel C. Reuman[7,8,*], and Guy Woodward[1,*].

[1] *Imperial College London, Silwood Park Campus, Buckhurst Road, Ascot, Berkshire SL5 7PY, UK.*

[2] *Research Center for Engineering Ecology and Nonlinear Science, North China Electric Power University, Beijing, 102206, China.*

[3] *School of Biological and Chemical Sciences, Queen Mary University of London, Mile End Road, London E1 4NS, UK.*

[4] *NIVA, Norwegian Institute for Water Research, Gaustadalléen 21, NO-0349 Oslo, Norway.*

[5] *German Centre for Integrative Biodiversity Research (iDiv) Halle-Jena-Leipzig, Deutscher Platz 5, 04103 Leipzig, Germany.*

[6] *Institute of Ecology, Friedrich Schiller University Jena, Dornburger Str. 159, 07743 Jena, Germany.*

[7] *University of Kansas, Department of Ecology and Evolutionary Biology and Kansas Biological Survey, 2041 Haworth Hall 1200 Sunnyside Avenue Lawrence, Kansas 66045, USA.*

[8] *Laboratory of Populations, Rockefeller University, New York, NY, 10065, USA.*

Classification: Biological Sciences – Ecology

Type of article: Letter

† These authors contributed equally to this work

*** Corresponding authors:** Eoin O'Gorman (e.ogorman@imperial.ac.uk), Daniel Reuman (reuman@ku.edu), Guy Woodward (guy.woodward@imperial.ac.uk)

Natural ecosystems typically consist of many small and few large organisms[1-4]. The scaling of this negative relationship between body mass and abundance has important implications for resource partitioning and energy usage[5-7]. Global warming over the next century is predicted to favour smaller organisms[8-12], producing steeper mass-abundance scaling[13] and a less efficient transfer of biomass through the food web[5]. Here, we show that the opposite effect occurs in a natural warming experiment involving 13 whole-stream ecosystems within the same catchment, which span a temperature gradient of 5-25 °C. We introduce a mechanistic model that shows how the temperature dependence of basal resource carrying capacity can account for these previously unexpected results. If nutrient supply increases with temperature to offset the rising metabolic demand of primary producers, there will be sufficient resources to sustain larger consumers at higher trophic levels. These new data and the model that explains them highlight important exceptions to some commonly assumed "rules" about responses to warming in natural ecosystems.

Body mass (*M*) is a key determinant of many ecological phenomena[6,7,14] (*e.g.* growth, metabolism, feeding) and its relationship with abundance (*N*) at either the individual or species level is well described by a simple power law, $N \propto M^b$ (hereafter "*MN*-scaling"). The exponent *b* and its controlling factors have generated considerable interest in community ecology for decades[4,6], with widespread recognition that *b* is related to energy flow through food webs[5-7]. Many studies have found that *MN*-scaling is conserved in the face of biodiversity loss or species turnover and so may be a relatively stable property of ecosystems[1-3]. Thus, a change in *MN*-scaling may highlight a fundamental disruption to the processes that govern energy flow through an ecosystem by environmental or anthropogenic stressors. For example, steepening of size-spectra (*i.e.* a more negative exponent *b*) following fisheries exploitation is indicative of widespread losses at higher trophic levels[5,15].

Key processes that could lead to altered *MN*-scaling include species extinctions or invasions, altered bottom-up or top-down control, changes in growth rate or reproductive output, and evolutionary adaptation to new environments. Population dynamical models predict that large organisms from higher trophic levels will go extinct first in warmer environments[16,17] because there is less energy available to them[14], with empirical support from microcosm experiments[11,17]. The theoretical basis for warming-induced changes in size structure at lower trophic levels is less well-developed[18,19], but there is widespread evidence for an increased prevalence of smaller organisms with warming[8-10], albeit with variability depending on the size-range and ecosystem considered[10,12]. Fewer large and more small organisms should result in steeper *MN*-scaling, as demonstrated in experimental ponds where warming favoured smaller phytoplankton and led to steeper size-spectra[13].

We tested the generality of this predicted temperature effect on *MN*-scaling across 13 Icelandic streams that span a natural temperature gradient of 5-25 °C (Fig. 1a), but are otherwise very similar in their physical and chemical properties[20-24]. Natural experiments and space-for-time substitutions have some limitations (*e.g.* non-random allocation of temperature "treatments", no observation of the warming process but rather its end point; see Supplementary Methods for discussion of these limitations), however, the streams occur in the same catchment and thus are free of the usual confounding effects of biogeographical differences or other environmental gradients[23,25]. The constituent species are a subset of those commonly found in continental Europe and North America[23], with compositional differences between the streams reflecting the local filtering of cold-stenotherms, warm-stenotherms, and eurytherms from the regional species pool[22]. The streams are thus an invaluable natural experiment for improving our ecosystem-level understanding of warming impacts[23,25].

Individual organisms were measured and counted from every stream (n = 13,085 individuals) to estimate the mean body mass and total abundance of each species (see

Methods). There was an interactive effect of body mass and stream temperature on abundance, *i.e*. temperature altered *MN*-scaling (Table 1). Contrary to traditional theoretical predictions, the exponent *b* became less negative as temperature increased (Fig. 1b,c; Fig. S1). This shallowing of *MN*-scaling was driven by differences across streams in two major trophic groups: primary producers and invertebrate consumers. Among the former, the abundance (Fig. 1d) and biomass (Fig. S2g) of diatoms decreased with temperature, contrary to the species shift hypothesis that warming should increase the abundance of small species[8]. Manipulative experiments suggest that this may be due to greater top-down control by grazers[22]. The mean body mass of invertebrates increased with temperature (Fig. 1e), in diametric opposition to the community body size shift hypothesis[8]. This was largely driven by compositional changes, with bigger species (such as the snail, *Radix balthica*) only occurring in warmer streams and dominating those communities[21-23].

The temperature effect on *MN*-scaling still held after quantifying only the mean body mass and total abundance of the major trophic groups (Table S1; Fig. S3), including additional data for cryptic biota that are typically overlooked and rarely quantified in freshwater studies (Table S2; Fig. S4), and excluding data for the apex fish predator, brown trout (*Salmo trutta*), which only occurs in the warmer streams (Tables 1, S1, and S2; Fig. 1c). Our findings were also robust to various methodological approaches, including different methods of averaging (Table S3; Fig. S5), regression model selection (Table S4; Fig. S6), and binning by individual size data (Table S5; Fig. S7). We focused on diatoms as the key primary producers in the system, but analysis of total chlorophyll (including diatoms, cyanobacteria, and green algae) did not alter our conclusions about the effect of temperature on the biomass of primary producers (Fig. S8).

To explain these apparent contradictions with established theory, we hypothesised that the equilibrium biomass of basal resources in the absence of consumption (*i.e*. the carrying

capacity, *K*) could play a critical role. For algae, *K* is determined by the balance between nutrient supply and demand[14,26]. Our study streams are co-limited by nitrogen and phosphorus, with nitrogen being the key limiting nutrient[21], *i.e*. the demand for nutrients will predominantly be met by the nitrogen and phosphorus cycles and input of these elements from groundwater or terrestrial sources. For autotrophs, the metabolic demand for nutrients is equal to the rate of photosynthesis[14]. To assess the upper and lower bounds of what is feasible in our system, we tested two extreme scenarios[26] for the temperature dependence of *K*: (*i*) if nutrient supply is constant, *K* should decrease with increasing temperature to exactly balance the increasing photosynthetic rate, *i.e*. with an activation energy, E_K, of -0.70 to -0.96, representing the inverse of the 95% confidence intervals (CI) of published temperature dependencies for photosynthesis in aquatic microalgae (see Supplementary Methods and Table S6); and (*ii*) if nutrient supply increases with temperature to a level that exactly matches the photosynthetic rate, *K* should be independent of temperature, *i.e*. $E_K = 0$.

Three lines of evidence suggest that the rate of nutrient supply increases with temperature in our system: (*i*) nitrogen fixation increases dramatically with temperature[27]; (*ii*) water-column concentrations of nutrients are not depleted with temperature[20-24], as would be expected due to the rising metabolic demand of primary producers if nutrient supply were constant; and (*iii*) the body mass of diatoms does not decrease with temperature[20] (Fig. S2d), as would be expected if competition for nutrients were strong[19]. Additionally, headwater streams are among the most metabolically active freshwaters due to regular replenishment of nutrients from surface to sub-surface exchanges[28]. Many headwater streams also exhibit biogeochemical steady state along their entire length, with nutrient inputs balancing outputs and nutrient concentrations similar to those of soil and groundwater[29]. Thus, we hypothesise that the temperature dependence of *K* cannot be entirely driven by the photosynthetic rate in our system, and that E_K determines *MN*-scaling.

We tested this hypothesis using a bioenergetic population dynamical model, which contains free parameters for the growth rate and K of primary producers, the metabolic and attack rates of invertebrates and fish, and estimates of the measurement error for the biomass of each trophic group (see Methods). We determined the combination of parameters that best fitted our empirical data using maximum likelihood. The optimum model explained 32%, 84%, and 97% of the variation across streams in the empirical biomass of diatoms, invertebrates, and fish, respectively (Fig. 2a), and had estimates for most parameters that overlapped with published values from other freshwater ecosystems (Table S7). The value of E_K that best described our data was -0.30, with 95% CI of -0.47 and 0.20. This range does not overlap with the 95% CI of E_K predicted for a constant nutrient supply (-0.70 to -0.96; Table S6), so we reject the null hypothesis that E_K is entirely driven by the photosynthetic rate.

We carried out a sensitivity analysis to determine the effect of E_K on *MN*-scaling. Here, we fixed all the parameter values from our best-fitting model except for E_K, which we varied from -1 to 0.5. The predicted steepening of *MN*-scaling with increasing temperature only occurred for $E_K < -0.33$, with the observed shallowing of *MN*-scaling found when $E_K > -0.33$ (Fig. 2b). This suggests that E_K plays a critical role in determining the effect of temperature on *MN*-scaling, *i.e*. the rate at which nutrient supply increases with temperature can offset the increasing photosynthetic rate, supporting a higher than expected K of basal resources and thus larger biomass of consumers.

The 5-25 °C temperature gradient of our streams is well within the thermal limits for survival of brown trout[30], so it is surprising that this fish species was only found > 15 °C (Fig. 2a), with similar results documented in a > 5 month fish tagging study from the system[31]. Our model can also help to understand these seemingly unexpected results. Resource production is converted to consumer production more efficiently as stream temperature increases[31] (Fig. S9). This may be driven by increasing dominance of *R. balthica*, which is the largest

herbivore in the system[21-23]. This highly efficient snail exerts stronger grazing pressure with increasing temperature[22] and thus may be a key conduit of energy flow to the fish. Mass-specific metabolic requirements are lower for larger organisms[14], so their population biomass should be higher, given the same amount of resources. Thus, we also hypothesised that the previously unexpected increase in the body mass of invertebrates with temperature (Fig. 1e) supported greater fish biomass in the warmer streams. We fixed all parameters at values from our best-fitting model, except for the temperature dependence of invertebrate body mass (E_{M2}) and, for each value of E_{M2}, determined the minimum model-predicted temperature at which fish were present in a stream. We found that the positive relationship between invertebrate body mass and temperature was critically important and that fish would not be supported if the relationship were negative, as predicted by temperature-size rules (Fig. 2c).

We have shown that the temperature dependencies of *K* and consumer body mass can modulate how warming affects energy flow through food webs in a previously unexpected manner. Thus, if resource production is sufficient in warmer environments, larger consumers may be sustained by a lower standing stock (*i.e.* abundance) of resources (Fig. 1c-e). While many of the studies investigating effects of temperature on the size structure of aquatic communities have focused on the lowest trophic level (*e.g.* microalgae)[9,20], our research highlights the potential for warming to alter the size distribution of unicells, ectothermic invertebrates, and vertebrates across > 12 orders of magnitude in body mass, and hence the flow of energy through the entire ecosystem. Larger apex predators have the potential to exert stronger top-down control, with effects that can cascade down to the lower trophic levels[32], but manipulative experiments would be needed to fully disentangle the direct effects of temperature from indirect effects due to stronger feeding at the top of the food web.

It is important to consider the context of our findings before attempting to generalise them to future impacts of climate change. The streams are quite species-poor, although the

key taxa are common throughout Europe and/or North America[23], so the results may be most relevant for Northern Hemisphere upland and/or headwater ecosystems with similarly low biodiversity. Our temperature gradient is substantial, with a range of 20 °C, which is more than twice the projected warming for tundra regions in the 21st century[33]. Nonetheless, the warmest stream is within the upper thermal tolerance of most freshwater invertebrate taxa[34]. As such, our results may be most relevant for ecosystems where constituent organisms are well below their thermal limits, *e.g.* at cool, high latitudes, where other exceptions to temperature-size rules have been identified[10], rather than in the tropics or warm temperate regions. For example, the thermal optimum for growth in brown trout is 11-19 °C (depending on resource quality[30]) and so there is scope for improved performance over part of the temperature range studied here[31]. The low productivity and nutrient-poor status of our streams[21,24] may also magnify the potential for increasing nutrient supply to offset higher metabolic demands at warmer temperatures. Nevertheless, our results contribute to a more general understanding of how warming could alter ecological communities because they suggest that changes in biomass at different trophic levels will depend on how the *K* of primary producers is affected by temperature, and this is an insight that can be tested broadly.

Our study system offers a powerful space-for-time substitution for warming impacts on natural communities, but also has limitations. Results from headwater streams may not scale up to larger ecosystems such as rivers, even though *MN*-scaling is consistently present across a broad range of ecosystems and common underlying mechanisms have been proposed[1,2,4,7]. Whilst we avoided biogeographical gradients that confound some studies, the close proximity of our streams could make it easier for organisms to disperse from the regional species pool to their optimum temperature than would be possible under a warming climate. Adaptation to warmer temperatures over many years of geothermal heating in the region may also produce different organismal responses relative to rapid climate change[25]. Nevertheless, a recent

whole-stream warming experiment from the system has revealed that changes in populations along the stream temperature gradient are similar to actual warming of a stream[35].

Our results show that warming effects on *MN*-scaling can hinge crucially on the temperature dependence of *K*, mediated through nutrient dynamics, at least in ecosystems with high production rates and strong trophic linkages. We need a broader understanding of how *K* depends on temperature in a range of environments (*e.g.* standing and flowing freshwaters, and marine and terrestrial ecosystems) to test the generality of our results further. Our data indicate that temperature-size rules, widely appreciated for their ubiquity[8-10], do not apply universally in natural communities, with important implications for the higher trophic levels. Our results improve our understanding of the contingencies in temperature effects on natural ecosystems, which should enhance our ability to predict the ecological consequences of future climate change.

Acknowledgements:

We thank Julia Reiss for meiofauna and protist data, Nicola Craig for laboratory work, Aristides Moustakas for advice on data analysis, Gísli Már Gíslason and Jón S. Ólafsson for providing research support and facilities, and Gabriel Yvon-Durocher, Samraat Pawar, Mark Trimmer, and Becca Kordas for helpful comments on earlier drafts. We acknowledge funding from NERC (NE/I009280/2, NE/F013124/1, NE/L011840/1, NE/M020843/1), the Royal Society (RG140601), the British Ecological Society (4009-4884), the National Special Water Program (No. 2009ZX07210-009), the China Scholarship Council (No. 201206730022), the Department of Environmental Protection of Shandong Province (SDHBPJ-ZB-08), the German Research Foundation (FZT 118), the James S. McDonnell Foundation, and NSF (1442595).

Author Contributions:

GW, NF, and DCR were responsible for funding application, research design, and planning. EOG, DEP, GA, and AS collected the data. EOG, BCR, and LZ analysed the data. LZ, DCR, and HZ did the modelling. All authors wrote the paper.

References:

1 Jonsson, T., Cohen, J. E. & Carpenter, S. R. Food webs, body size, and species abundance in ecological community description. *Advances in Ecological Research* **36**, 1-84 (2005).

2 Marquet, P. A., Navarrete, S. A. & Castilla, J. C. Scaling population-density to body size in rocky intertidal communities. *Science* **250**, 1125-1127 (1990).

3 O'Gorman, E. J. & Emmerson, M. C. Body mass-abundance relationships are robust to cascading effects in marine food webs. *Oikos* **120**, 520-528 (2011).

4 Reuman, D. C., Mulder, C., Raffaelli, D. & Cohen, J. E. Three allometric relations of population density to body mass: theoretical integration and empirical tests in 149 food webs. *Ecology Letters* **11**, 1216-1228 (2008).

5 Jennings, S. & Blanchard, J. L. Fish abundance with no fishing: predictions based on macroecological theory. *Journal of Animal Ecology* **73**, 632-642 (2004).

6 White, E. P., Ernest, S. K. M., Kerkhoff, A. J. & Enquist, B. J. Relationships between body size and abundance in ecology. *Trends in Ecology & Evolution* **22**, 323-330 (2007).

7 Woodward, G. *et al.* Body size in ecological networks. *Trends in Ecology & Evolution* **20**, 402-409 (2005).

8 Daufresne, M., Lengfellner, K. & Sommer, U. Global warming benefits the small in aquatic ecosystems. *Proceedings of the National Academy of Sciences of the United States of America* **106**, 12788-12793 (2009).

9 Moran, X. A. G., Lopez-Urrutia, A., Calvo-Diaz, A. & Li, W. K. W. Increasing importance of small phytoplankton in a warmer ocean. *Global Change Biology* **16**, 1137-1144 (2010).

10 Sheridan, J. A. & Bickford, D. Shrinking body size as an ecological response to climate change. *Nature Climate Change* **1**, 401-406 (2011).

11 Petchey, O. L., McPhearson, P. T., Casey, T. M. & Morin, P. J. Environmental warming alters food-web structure and ecosystem function. *Nature* **402**, 69-72 (1999).

12 Gardner, J. L., Peters, A., Kearney, M. R., Joseph, L. & Heinsohn, R. Declining body size: a third universal response to warming? *Trends in Ecology & Evolution* **26**, 285-291 (2011).

13 Yvon-Durocher, G., Montoya, J. M., Trimmer, M. & Woodward, G. Warming alters the size spectrum and shifts the distribution of biomass in freshwater ecosystems. *Global Change Biology* **17**, 1681-1694 (2011).

14 Brown, J. H., Gillooly, J. F., Allen, A. P., Savage, V. M. & West, G. B. Toward a metabolic theory of ecology. *Ecology* **85**, 1771-1789 (2004).

15 Rice, J. & Gislason, H. Patterns of change in the size spectra of numbers and diversity of the North Sea fish assemblage, as reflected in surveys and models. *ICES Journal of Marine Science* **53**, 1214-1225 (1996).

16 Binzer, A., Guill, C., Brose, U. & Rall, B. C. The dynamics of food chains under climate change and nutrient enrichment. *Philosophical Transactions of the Royal Society of London B: Biological Sciences* **367**, 2935-2944 (2012).

17 Fussmann, K. E., Schwarzmüller, F., Brose, U., Jousset, A. & Rall, B. C. Ecological stability in response to warming. *Nature Climate Change* **4**, 206-210 (2014).

18 DeLong, J. P. Experimental demonstration of a 'rate–size'trade-off governing body size optimization. *Evolutionary Ecology Research* **14**, 343-352 (2012).

19 Reuman, D. C., Holt, R. D. & Yvon-Durocher, G. A metabolic perspective on competition and body size reductions with warming. *Journal of Animal Ecology* **83**, 59-69 (2014).

20 Adams, G. *et al.* Diatoms can be an important exception to temperature-size rules at species and community levels of organization. *Global Change Biology* **19**, 3540-3552 (2013).

21 Friberg, N. *et al.* Relationships between structure and function in streams contrasting in temperature. *Freshwater Biology* **54**, 2051-2068 (2009).

22 O'Gorman, E. J. *et al.* Impacts of warming on the structure and function of aquatic communities: individual- to ecosystem-level responses. *Advances in Ecological Research* **47**, 81-176 (2012).

23 Woodward, G. *et al.* Sentinel systems on the razor's edge: effects of warming on Arctic geothermal stream ecosystems. *Global Change Biology* **16**, 1979-1991 (2010).

24 Demars, B. O. L. *et al.* Temperature and the metabolic balance of streams. *Freshwater Biology* **56**, 1106-1121 (2011).

25 O'Gorman, E. J. *et al.* Climate change and geothermal ecosystems: natural laboratories, sentinel systems, and future refugia. *Global Change Biology* **20**, 3291-3299 (2014).

26 Gilbert, B. *et al.* A bioenergetic framework for the temperature dependence of trophic interactions. *Ecology Letters* **17**, 902-914 (2014).

27 Welter, J. R. *et al.* Does N2-fixation amplify the temperature dependence of ecosystem metabolism? *Ecology* **96**, 603-610 (2015).

28 Battin, T. J. *et al.* Biophysical controls on organic carbon fluxes in fluvial networks. *Nature Geosci* **1**, 95-100 (2008).

29 Brookshire, E., Valett, H. & Gerber, S. Maintenance of terrestrial nutrient loss signatures during in-stream transport. *Ecology* **90**, 293-299 (2009).

30 Elliott, J. & Elliott, J. Temperature requirements of Atlantic salmon Salmo salar, brown trout Salmo trutta and Arctic charr Salvelinus alpinus: predicting the effects of climate change. *Journal of Fish Biology* **77**, 1793-1817 (2010).

31 O'Gorman, E. J. *et al.* Temperature effects on fish production across a natural thermal gradient. *Global Change Biology* **22**, 3206-3220 (2016).

32 Kratina, P., Greig, H. S., Thompson, P. L., Carvalho-Pereira, T. S. & Shurin, J. B. Warming modifies trophic cascades and eutrophication in experimental freshwater communities. *Ecology* **93**, 1421-1430 (2012).

33 IPCC. *Working Group I contribution to the IPCC fifth assessment report. Climate change 2013: the physical sciences basis summary for policymakers*. 36 (Cambridge University Press, 2013).

34 Stewart, B. A., Close, P. G., Cook, P. A. & Davies, P. M. Upper thermal tolerances of key taxonomic groups of stream invertebrates. *Hydrobiologia* **718**, 131-140 (2013).

35 Nelson, D. *et al.* Experimental whole-stream warming alters community size structure. *Global Change Biology* (2016).

Table 1. Statistical output from linear mixed effects (LME) models. Ln-species abundance (m^{-2}) was the dependent variable, ln-mean species body mass (mg) and stream temperature (°C) were fixed effects, and species identity was a random effect. Data were for 13 streams in August 2008 including diatoms, macroinvertebrates, and fish. Summary tables for analyses (a) including and (b) excluding the apex fish predator are presented, with model-predicted values, their standard errors (SE), degrees of freedom (DF), *t*-values, and *p*-values.

(a) LME including fish	**Value**	**SE**	**DF**	***t*-value**	***p*-value**
(Intercept)	2.7966	0.3747	527	7.463	<0.0001
mass	-0.7228	0.0277	527	-26.080	<0.0001
temperature	0.3814	0.2380	527	1.603	0.1096
mass × temperature	0.0591	0.0184	527	3.204	0.0014

(b) LME excluding fish	**Value**	**SE**	**DF**	***t*-value**	***p*-value**
(Intercept)	2.8084	0.3996	521	7.027	<0.0001
mass	-0.7221	0.0290	521	-24.882	<0.0001
temperature	0.4050	0.2510	521	1.614	0.1072
mass × temperature	0.0611	0.0194	521	3.153	0.0017

Figure Legends:

Fig. 1. Map of the geothermal streams and effects of temperature on mass-abundance (*MN*) scaling. a, mean daytime temperature in August 2008 for 13 geothermally heated streams in Hengill, Iceland. **b,** predicted and observed effects of increasing temperature on *MN*-scaling: more small organisms, fewer large organisms, and/or decreasing body size are predicted in warmer environments, leading to a steeper *MN* slope, but the opposite occurs in the Hengill streams. The dashed blue line is the *MN* relationship in the coldest stream, to act as a reference point for the warmest stream. **c,** the slope of the *MN* relationship, *b*, becomes shallower with increasing stream temperature. The solid and dashed lines are the results of the best-fitting models from analyses including and excluding fish, respectively (Table 1). The circles and crosses are the *MN* slopes for each stream from analyses including and excluding fish, respectively. **d,** ln-abundance of diatoms decreases with temperature (y = -0.740x + 19.46, $F_{1,11}$ = 20.18, p < 0.001, r^2 = 0.62). **e,** ln-body mass of invertebrates increases with temperature (y = 0.757x - 2.032 $F_{1,11}$ = 30.25, p < 0.001, r^2 = 0.71).

Fig. 2. A mechanistic model helps reveal the underlying processes of the stream ecosystems. a, the best-fitting model (solid lines) closely approximates the empirical biomass of the three major trophic groups in the Hengill streams (circles). **b,** influence of the activation energy of carrying capacity, E_K, on the slope of the *MN* relationship, *b*. A negative rate of change of *b* with respect to temperature ($°C^{-1}$) indicates a steepening of *MN*-scaling with warming as predicted by metabolic theory; this occurs for most negative values of E_K (*e.g*. bottom-right inset). A positive rate of change of *b* indicates a shallowing of *MN*-scaling, as observed in the empirical data; this only occurs for E_K > -0.33 (*e.g*. top-left inset). Circles indicate simulation results and solid lines are the fitted linear regressions. **c,** influence of the activation energy of invertebrate body mass, E_{M2}, on the minimum temperature at which fish

326 are present in a stream, T_m. The solid grey line indicates E_{M2} below which fish cannot invade
327 the system (E_{M2} = 0.744); the empirical value of E_{M2} is only marginally higher than this (E_{M2}
328 = 0.757). Values of E_{M2} beyond the dashed grey line are too large to be representative of the
329 data (E_{M2} = 1.925).
330

331 **Fig. 1**

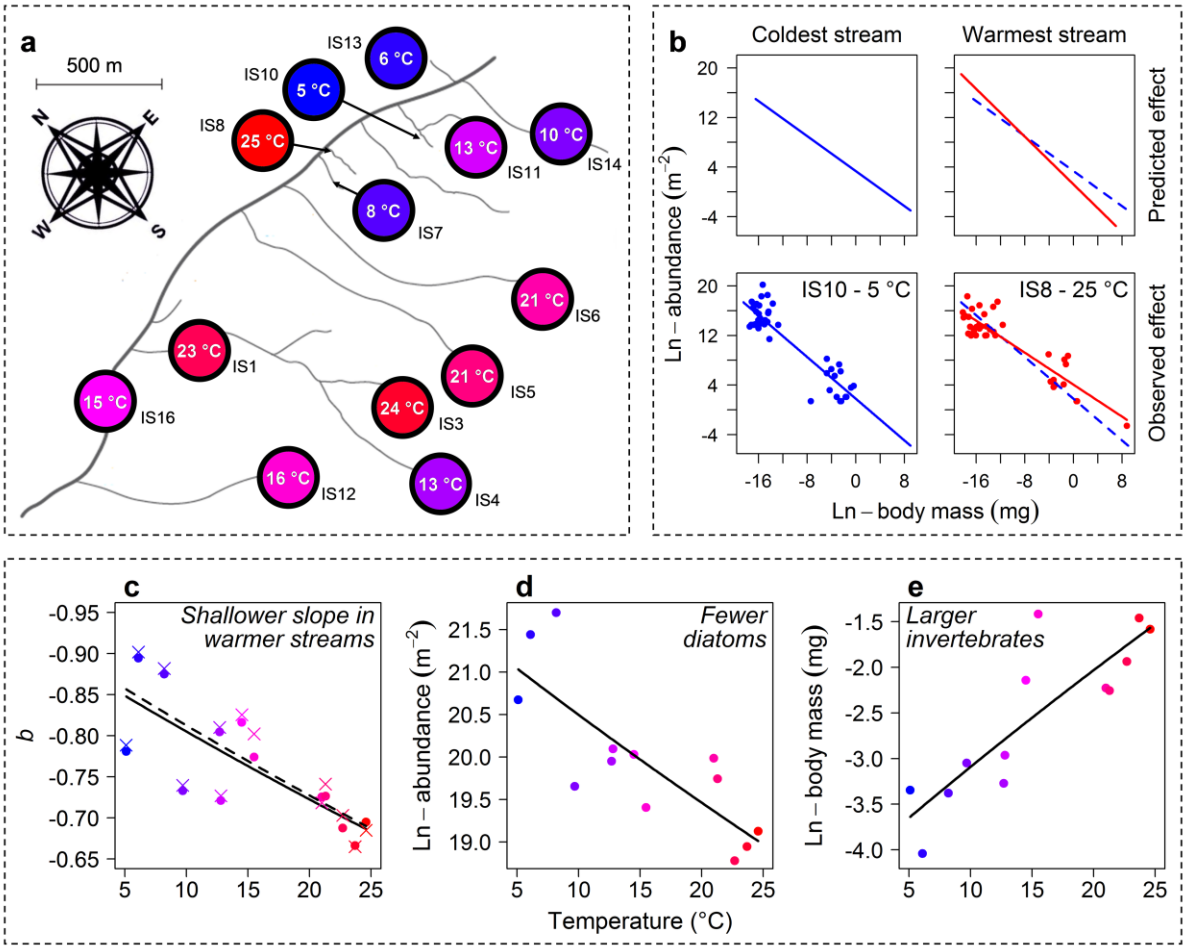
a
500 m
N
E
S
W
IS13
6 °C
IS10
5 °C
IS8
25 °C
13 °C
IS11
10 °C
IS14
8 °C
IS7
21 °C
IS6
23 °C
IS1
21 °C
IS5
15 °C
IS16
24 °C
IS3
16 °C
IS12
13 °C
IS4
b
Coldest stream
Warmest stream
Predicted effect
Observed effect
Ln – abundance (m^{-2})
IS10 - 5 °C
IS8 - 25 °C
Ln – body mass (mg)
c
Shallower slope in warmer streams
b
d
Fewer diatoms
Ln – abundance (m^{-2})
Temperature (°C)
e
Larger invertebrates
Ln – body mass (mg)

332

333 **Fig. 2**

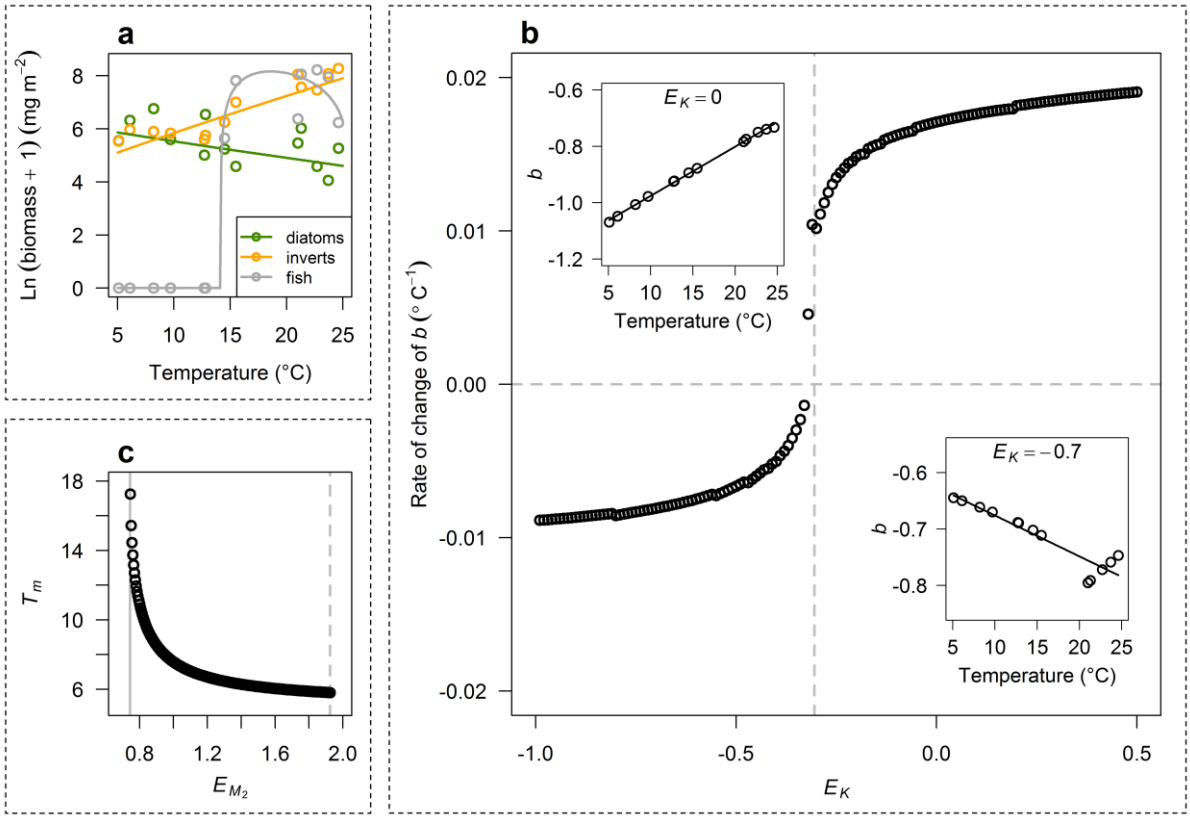
a
Ln (biomass + 1) (mg m^{-2})
Temperature (°C)
diatoms
inverts
fish
b
Rate of change of b (° C^{-1})
E_K
$E_K = 0$
$E_K = -0.7$
b
Temperature (°C)
c
T_m
E_{M_2}

334

Methods

Study site

Fieldwork was performed in August 2008 in the Hengill geothermal valley, Iceland (N 64°03; W 21°18), which has been intensively studied over the past decade[20-24,31,35-37]. We focused on 13 streams that occur within 1.5 km of each other and spanned a temperature gradient of 5-25 °C, which were also the minimum and maximum temperatures during the sampling period (see Table S8 and Supplementary Methods for more details). Note that most of the streams freeze over for part of the winter (Table S8), including several streams where fish are found (*e.g.* IS1, 3, and 12). There are also some streams that do not freeze which do not contain fish (*e.g.* IS13), suggesting that trout populations are not solely determined by winter freezing and are most likely sustained through interconnectivity with the main river[31]. Temperature differences between streams are due to groundwater that absorbs heat from the underlying bedrock, rather than direct upwelling of geothermal water and gases[38]. Thus, the streams have very similar water chemistry, with no confounding effects of temperature on pH, derivatives of nitrogen and phosphorus, and a wide range of other minerals and nutrients[20-24]. The streams are also very similar in their physical characteristics[21,24] and occur in a pristine mountain landscape, with no nutrient input or pollution from agriculture or industry. There are no trees or shrubs in the region, thus minimal coarse allochthonous input. The soil system exhibits a similar temperature gradient to the streams due to geothermal heating[31], thus nutrient inputs from the soil should not be decoupled from temperature effects on nutrient dynamics in the streams. The only other external influence on the streams may come from rare occurrences of terrestrial predators, such as the golden plover and Arctic fox, and grazing by sheep. The streams are thus an ideal natural experiment for studying the effects of warmer temperatures on the structure of freshwater communities[25] (but see Supplementary Methods for the strengths and weaknesses of natural experiments).

Diatom abundance and body mass estimation

Diatoms were collected from three stone scrapes per stream (noting the area of each stone) and preserved in Lugol's solution. Diatom frustules were cleared of organic matter with nitric acid, dried, and mounted on slides with naphrax. Abundances were estimated by counting the number of individuals of each species along a 15 × 0.1 mm transect of each slide, ensuring a transect contained at least 300 individuals. The number of stone scrapes, sample dilution, and transect and stone area were all used to calculate the abundance of each species (m^{-2}). Photographs of diatoms were taken with a Nikon Digital Sight DS-5M camera mounted on a Nikon Eclipse 50i microscope, or a high resolution digital SLR camera mounted on an Olympus BH2 microscope, at 1,000× magnification. Two linear dimensions were measured in Image J[39] for at least ten individuals (where available) of every diatom species in every stream, *i.e.* valve length and valve width in microns (n = 9,011 individuals from 69 different taxa). Every diatom species was assigned a shape corresponding to established methodologies[22,24] (Table S9). Cell biovolume (μm^3) was calculated according to associated biovolume formulae[40]. Cell carbon content was estimated from published cell volume to cell carbon relationships[41] and converted to dry mass (mg) assuming an average carbon by dry weight content of 19% per cell[42].

Macroinvertebrate abundance and body mass estimation

Macroinvertebrates were collected by taking five Surber samples (25 × 20 cm quadrat; 200 μm mesh) per stream and preserving them in 70% ethanol. The abundance of every invertebrate species was averaged across the five Surber samples and scaled by quadrat area (m^{-2}). Photographs of every invertebrate individual identified were taken with a Nikon Digital Sight DS-5M camera mounted on a Nikon Eclipse 50i or a Nikon SMZ1500 microscope, at

400-1,000× magnification for Chironomidae and 100× magnification for all other groups. One linear dimension was measured in Image J[39] for at least ten individuals (where available) of every invertebrate species in every stream (n = 4,121 individuals from 42 different taxa). Published length-weight relationships were used to estimate dry body mass (mg) from the linear measurements (Table S10).

Fish abundance and body mass estimation

Only one fish species is found in the system: the brown trout, *Salmo trutta*. Population abundances (m^{-2}) of this species were characterised using three-run depletion electrofishing of a 50 m reach within a stream, or the entire stream if less than 50 m in length[43]. Electrofishing of the entire catchment was carried out over a two day period. Body mass measurements of every fish (n = 53 individuals) were made on a portable mass balance (Ohaus Scout Pro Portable, 400 g capacity, 0.01 g accuracy). Dry mass (mg) of trout was calculated according to a wet weight to dry weight relationship established from 39 individuals of *S. trutta* ($y = 1.088x - 0.878$, $F_{1,37} = 1{,}201$, $p < 0.0001$, $r^2 = 0.97$). This fish species is orders of magnitude bigger than any other species in the streams and is thus the apex predator whenever it occurs. See Supplementary Methods for quantification of other trophic groups, including cryptic biota (meiofauna, ciliates, and flagellates) and unicellular algae other than diatoms (microscopic green algae and cyanobacteria).

Empirical exploration of MN-scaling

Population abundance should follow a power law with mean body mass[6] and an exponential relationship with temperature[14] as follows:

$$N = a_N M^{b_N} e^{E_N T_{arr}}, \quad (1)$$

Here, N is total species abundance (m^{-2}), a_N is a constant, b_N is the allometric exponent, M is mean species body mass (mg), E_N is the activation energy (eV), and T_{arr} is the standardised Arrhenius temperature:

$$T_{arr} = \frac{T - T_0}{kTT_0}, \quad (2)$$

where T is the absolute stream temperature (K), T_0 is an arbitrary reference temperature (293.15 K), and k is the Boltzmann constant (8.618×10^{-5} eV K^{-1}). We applied a natural logarithmic transformation to linearise the function in Equation 1 and added an interaction term to test our hypothesis that the allometric slope will change with increasing temperature:

$$\ln N = \ln a_N + b_N \ln M + E_N T_{arr} + c_N \ln M T_{arr}, \quad (3)$$

We analysed the data for all 13 streams with generalised least squares models and linear mixed effects models, using the '*gls*' and '*lme*' functions in the '*nlme*' package of R 3.2.0, with '*lmeControl*' parameters specified to deal with convergence issues (see R code in Supplementary Methods). Species identity was included as a random factor, to account for differences in community composition between streams[21-23]. Specifically, we accounted for the possibility that abundance could be different for each species (*i.e*. a random intercept) and that the effect of body mass and/or temperature on abundance could also be different for each species (*i.e*. random slopes). We compared models including the full fixed-effect structure plus all possible combinations of the random structure using both Aikake Information Criterion (AIC) and top-down hypothesis testing with the likelihood ratio test[44]. The random structure with species identity influencing a_N, b_N, and E_N, but not c_N, was identified as the best model using both approaches (ΔAIC > 2.39; p = 0.009 in a likelihood ratio test against the next best model). We used this structure in subsequent analyses, set '*method = "ML"* ' in the '*lme*' function, and performed AIC comparison and likelihood ratio tests on all possible combinations of the fixed-effect structure[44]. The full model (*i.e*. Equation 3) was identified as

433 the best model using both model selection approaches (ΔAIC > 6.57; p < 0.001 for the
434 interaction term in a likelihood ratio test).

435 Brown trout occur as the apex predator in a subset of streams[22] and are orders of
436 magnitude larger than all other species. To rule out the possibility that changes in *MN*-scaling
437 were solely driven by this large predator, we repeated the analysis with this species excluded.
438 We carried out all the same model selection procedures as above. The best-fitting model once
439 again contained the random structure with species identity influencing a_N, b_N, and E_N, but not
440 c_N, (ΔAIC > 2.36; p = 0.010 in a likelihood ratio test against the next best model) and the full
441 fixed-effect structure (ΔAIC > 6.42; p = 0.019 for the interaction term in a likelihood ratio
442 test). For both analyses, we set '*method = "REML"* ' before extracting model summaries and
443 partial residuals from the best-fitting model[44]. Note that the models were always fitted to the
444 raw data collected from the streams, with residuals only extracted for a visual representation
445 of the best-fitting models, excluding the noise explained by the random effect of species
446 identity (see R code in Supplementary Methods).

447

448 *Trophic group biomass and trophic transfer efficiency*

449 To determine the proximate drivers of the observed changes across the temperature
450 gradient in *MN*-scaling, associations with temperature of the total abundance (m^{-2}),
451 abundance-weighted mean body mass (mg), and total biomass (mg m^{-2}) of diatoms,
452 invertebrates, and fish were explored with linear regression analysis. We also calculated a
453 predicted metric of trophic transfer efficiency, *TE*, to determine whether the observed
454 changes in *MN*-scaling with temperature altered the energy flow through the system:

455 $$\ln TE = (b_1 - b_0) \ln MR, \quad (4)$$

456 where b_1 is the *MN* slope from a given stream, b_0 is the *MN* slope of -0.75 predicted for
457 ecosystems in which the biota share a common energy source[6,45], and *MR* is the consumer-

458 resource body mass ratio[46]. *MR* was estimated using mean species body mass values and
459 consumer-resource feeding links previously established for the Hengill system[22]. The
460 temperature dependencies of *MR* and *TE* were explored with linear regression analysis. Note
461 that all linear regressions in the study were performed according to the equation:

462 $$\ln RV = \ln a_{RV} + E_{RV} T_{arr}, \quad (5)$$

463 where *RV* is the response variable of interest (either *MR*, *TE*, chlorophyll, or the total
464 abundance, abundance-weighted mean body mass, or total biomass of each trophic group)
465 and all other terms are the same as in Equation 3.

466

467 *Bioenergetic model*

468 We constructed a bioenergetic population dynamical model to describe the dynamical
469 change of the three main trophic groups in Hengill: diatoms (group 1), invertebrates (group
470 2), and fish (group 3). These trophic groups form a food chain, and the change of their
471 biomasses through time was modelled as follows:

472 $$\frac{dB_1}{dt} = rB_1\left(1 - \frac{B_1}{K}\right) - y_2 B_1 B_2 \quad (6a)$$

473 $$\frac{dB_2}{dt} = e_2 y_2 B_1 B_2 - x_2 B_2 - y_3 B_2 B_3 \quad (6b)$$

474 $$\frac{dB_3}{dt} = e_3 y_3 B_2 B_3 - x_3 B_3 \quad (6c)$$

475 Here, B_1, B_2, and B_3 denote the biomass of diatoms, invertebrates, and fish, respectively (mg
476 m^{-2}); r is the maximum mass-specific growth rate of diatoms (day^{-1}); K is the carrying
477 capacity (mg m^{-2}); x_i is the mass-specific metabolic rate of trophic group i (day^{-1}); y_i
478 represents the attack rate of trophic group i (m^2 mg^{-1} day^{-1}); e_2 = 0.45 is the assimilation
479 efficiency when invertebrates consume diatoms[47]; and e_3 = 0.85 is the assimilation efficiency
480 when fish consume invertebrates[47]. In simple terms, this model estimates changes in the

biomass of: (1) diatoms, as their growth (determined by r and K) minus their consumption by invertebrates (determined by y_2); (2) invertebrates, as the assimilated proportion of the diatom biomass that they consume (determined by e_2 and y_2), minus their metabolic demand (determined by x_2), minus their consumption by fish (determined by y_3); and (3) fish, as the assimilated proportion of the invertebrate biomass that they consume (determined by e_3 and y_3), minus their metabolic demand (determined by x_3).

Based on the metabolic theory of ecology[14,48], the parameters r, K, x, and y are related to body mass and temperature as follows:

$$r = a_r M_i^{b_r} e^{E_r T_{arr}}, \; i = 1, \tag{7a}$$

$$K = a_K M_i^{b_K} e^{E_K T_{arr}}, \; i = 1, \tag{7b}$$

$$x_i = a_{x_i} M_i^{b_{x_i}} e^{E_{x_i} T_{arr}}, \; i = 2 \text{ or } 3, \tag{7c}$$

$$y_i = a_{y_i} M_i^{b_{y_i}} M_j^{c_{y_i}} e^{E_{y_i} T_{arr}}, \; i = 2 \text{ or } 3, \; j = i\text{-}1. \tag{7d}$$

Here, a_r, a_K, a_{xi}, and a_{yi} are the allometric constants, b_r, b_K, b_{xi}, and b_{yi} are the allometric exponents, and E_r, E_K, E_{xi}, and E_{yi} are the activation energies describing the Arrhenius increase in growth rate, carrying capacity, metabolic rate, and attack rate of trophic group i with temperature, respectively (eV); c_{yi} is the allometric exponent for the resource one trophic level below trophic group i; and M_i is the mean body mass of trophic group i (mg). We used the abundance-weighted mean trophic group body mass for diatoms ($M_1 = 5.8340\times10^{-7}$ mg) and fish ($M_3 = 9.4854\times10^{3}$ mg) because they do not vary systematically with temperature (Fig. S2d,f). The body mass of invertebrates increases with temperature, so we used the following equation to estimate the mean body mass of invertebrates (mg) at each stream temperature:

$$\ln M_2 = \ln a_{M_2} - E_{M_2} T_{arr}, \tag{8}$$

where E_{M2} = 0.757 and ln a_{M2} = -2.032 (Fig. S2e). Note that we carried out a dimensionality reduction to avoid parameter redundancy in the model (see Supplementary Methods and Tables S11 and S12).

Likelihood function

We performed a stability analysis to determine the conditions under which the equilibrium points of the model are stable (see Supplementary Methods). This analysis indicated that for any set of model parameters there was a unique stable equilibrium of the dynamical model for each stream, which provided the model-predicted biomass values for the stream, for those parameters. If z_i^{diatom} is the model-predicted ln-biomass of diatoms and $Z_{i,j}^{diatom}$ are the three stone scrape measurements of the ln-biomass of diatoms in stream *i*, we assumed the residuals $\varepsilon = z_i^{diatom} - Z_{i,j}^{diatom}$ should follow a normal distribution with mean 0 and standard deviation δ_{diatom}. These were always finite because diatoms were present in all streams and because all potentially stable equilibria of the dynamical model predicted diatom populations > 0. The log likelihood for diatoms for all 13 streams was then taken to be:

$$\ln L_{all}^{diatom} = \sum_{i=1}^{13}\sum_{j=1}^{3}\left(-\frac{1}{2}\ln(2\pi) - \ln\delta_{diatom} - \frac{\left(z_i^{diatom} - Z_{i,j}^{diatom}\right)^2}{2\delta_{diatom}^{\ 2}}\right). \quad (9a)$$

We followed an analogous procedure for invertebrates and fish, except we had to accommodate the case in which model-predicted or observed densities were zero. Since invertebrates were observed in all streams, we took the log likelihood for invertebrates to be -∞ if invertebrates were predicted by the model to be absent from any stream, and otherwise:

$$\ln L_{all}^{invert} = \sum_{i=1}^{13}\sum_{j=1}^{5}\left(-\frac{1}{2}\ln(2\pi) - \ln\delta_{invert} - \frac{\left(z_i^{invert} - Z_{i,j}^{invert}\right)^2}{2\delta_{invert}^{\ 2}}\right), \quad (9b)$$

where z_i^{invert} is the model-predicted ln-biomass of invertebrates and $Z_{i,j}^{invert}$ are the five Surber

sample measurements of the ln-biomass of invertebrates in stream *i*. For fish, we took the log likelihood to be $-\infty$ if fish were predicted by the model to be absent from any of the streams in which they were actually observed, or predicted by the model to be present in any of the streams in which they were not observed, and otherwise:

$$\ln L_{all}^{fish} = \sum_{i \in I} \left(-\frac{1}{2} \ln(2\pi) - \ln \delta_{fish} - \frac{\left(z_i^{fish} - Z_i^{fish} \right)^2}{2 \delta_{fish}^{\ 2}} \right), \quad (9c)$$

where I is the set of seven streams in which fish were observed, z_i^{fish} is the model-predicted ln-biomass of fish, and Z_i^{fish} are the values of fish ln-biomass estimated from three-run depletion electrofishing in stream *i*.

Finally, we can get the joint log likelihood for all three groups in the 13 streams:

$$\ln L = \ln L_{all}^{diatom} + \ln L_{all}^{invert} + \ln L_{all}^{fish} \quad (10)$$

This likelihood function corresponds to a statistical model based on sampling log populations from normal distributions centred at equilibrium log population values from the dynamical model, except that when dynamical-model population equilibria are zero, only a sample population estimate of zero is possible. The procedure for dealing with numeric difficulties caused by parameters which yield a value of -∞ is described in Supplementary Methods.

Optimisations

After dimensionality reduction (see Supplementary Methods), there were 13 parameters to be determined in our model, so we sampled 10,000 different starting parameter combinations from the 13-dimensional hypercube in which each parameter ranged from -100 to 100 using a Sobol sequence (with the '*sobolset*' function in Matlab 7.12.0). We optimised likelihood for each set and chose the combination of optimised parameters that gave the maximal likelihood (with the '*fminsearchcon*' function in Matlab). We then used these values

as the initial point of 2,000,000 iterations in our subsequent Markov Chain Monte Carlo (MCMC) simulations, which were carried out using the Filzbach package in Microsoft Visual C++ 2010. Filzbach provides a convergence statistic for MCMC chains, with values close to 1 suggesting mean chain convergence and values > 1.2 indicating mean non-convergence. The value for our simulations was 1.007. We chose the highest-likelihood parameters ever obtained in this process as the optimised values for each of the 13 parameters in our model (see Table S7). This was entirely a maximum likelihood approach, with MCMC used as an aid to optimisation and as a tool for producing confidence intervals (through profiling), rather than in a hybrid Bayesian fashion. Confidence intervals are those returned by Filzbach. The reason for using both '*fminsearchcon*' and MCMC to help optimise was that they have complementary strengths in rapid convergence to a local maximum and broad exploration of the likelihood surface, respectively. Model validation is described in the Supplementary Methods.

Additional References:

36 Gudmundsdottir, R. *et al.* Effects of temperature regime on primary producers in Icelandic geothermal streams. *Aquatic Botany* **95**, 278-286 (2011).

37 Hannesdóttir, E. R., Gíslason, G. M., Ólafsson, J. S., Ólafsson, Ó. P. & O'Gorman, E. J. Increased stream productivity with warming supports higher trophic levels. *Advances in Ecological Research* **48**, 283-340 (2013).

38 Arnason, B., Theodorsson, P., Björnsson, S. & Saemundsson, K. Hengill, a high temperature thermal area in Iceland. *Bulletin of Volcanology* **33**, 245-259 (1969).

39 Abramoff, M. D., Magalhaes, P. J. & Ram, S. J. Image processing with ImageJ. *Biophotonics International* **11**, 36-42 (2004).

40 Sun, J. & Liu, D. Geometric models for calculating cell biovolume and surface area for phytoplankton. *Journal of Plankton Research* **25**, 1331-1346 (2003).

41 Rocha, O. & Duncan, A. The relationship between cell carbon and cell volume in freshwater algal species used in zooplanktonic studies. *Journal of Plankton Research* **7**, 279-294 (1985).

42 Sicko-Goad, L. M., Schelske, C. L. & Stoermer, E. F. Estimation of intracellular carbon and silica content of diatoms from natural assemblages using morphometric techniques. *Limnology and Oceanography* **29**, 1170-1178 (1984).

43 Seber, G. A. F. & Le Cren, E. D. Estimating population parameters from catches large relative to the population. *Journal of Animal Ecology* **36**, 631-643 (1967).

44 Zuur, A. F., Ieno, E. N., Walker, N. J., Saveliev, A. A. & Smith, G. M. in *Mixed effects models and extensions in ecology with R* 101-142 (Springer, 2009).

45 Damuth, J. Population-density and body size in mammals. *Nature* **290**, 699-700 (1981).

46 Jennings, S. & Mackinson, S. Abundance–body mass relationships in size-structured food webs. *Ecology Letters* **6**, 971-974 (2003).

47 Yodzis, P. & Innes, S. Body size and consumer-resource dynamics. *American Naturalist*, 1151-1175 (1992).

48 Vasseur, D. A. & McCann, K. S. A mechanistic approach for modeling temperature-dependent consumer-resource dynamics. *American Naturalist* **166**, 184-198 (2005).